Spatiotemporal Lineage Tracing Reveals Molecular and Spatial Heterogeneity in Cochlear Sensory Epithelium

Mingxuan Wu[1,2,3,4#], Jiacheng Fan[6#], Yuyan Gu[1], Yuqiu Zhou[6], Tianshi Sun[7], Yaoqian Liu[1,2,3,4], Gaogan Jia[1,2,3,4], Jinjie Yang[7], Yiyun Lou[1,2,3,4], Yunjie Li[1,2,3,4], Huawei Li[1,2,3,4,5], Wenquan Li[8]*, Yan Chen[1]*, Ying Zhu[6]*, Wenyan Li[1,2,3,4,5]*

Supplementary Legends

Figure S1

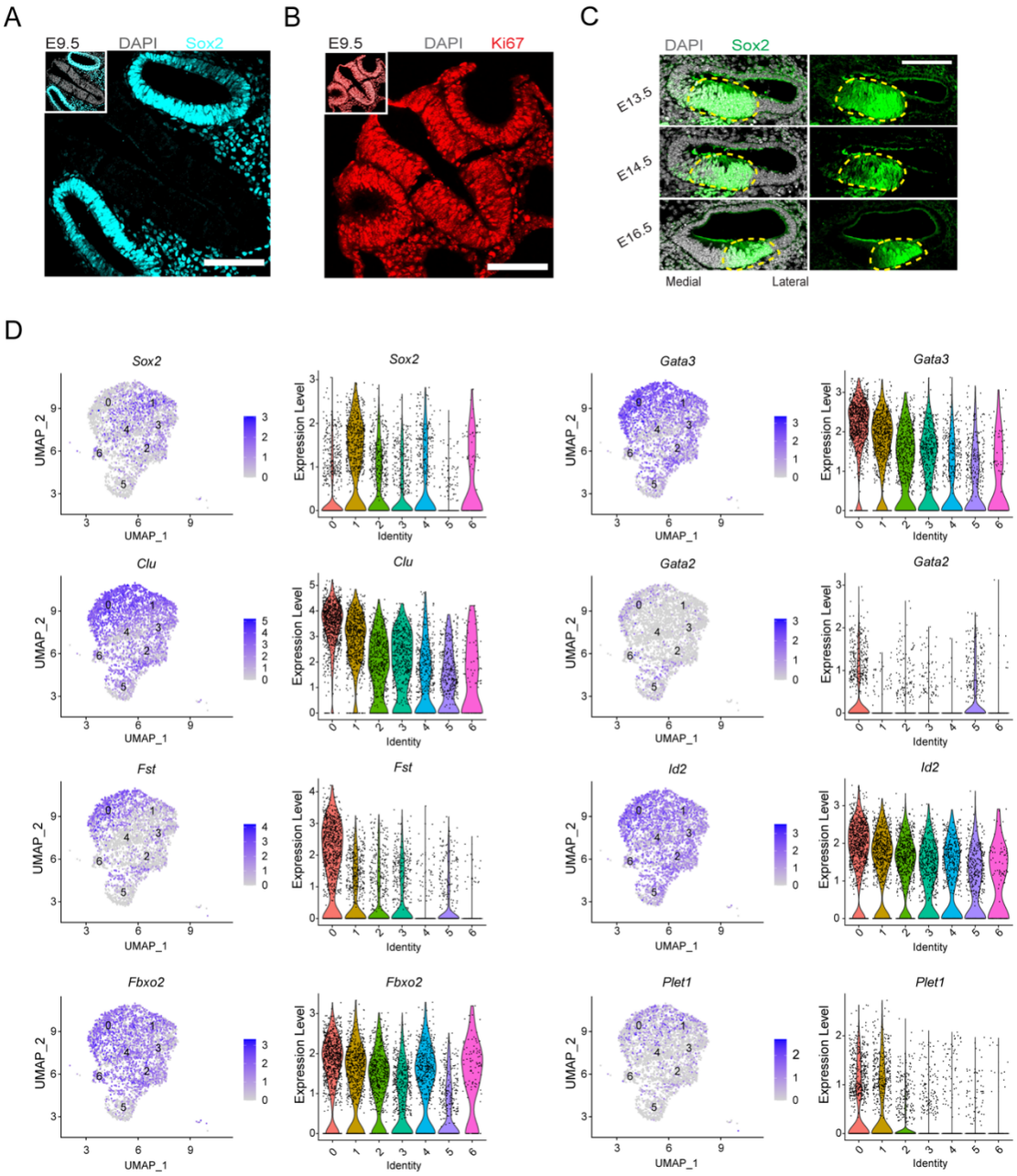


Figure S1. Morphogenetic Remodeling and Cellular Heterogeneity in the Developing Mouse Cochlear Epithelium.

(A, B) Expression patterns of SOX2 and KI67 in the E9.5 otocyst. Scale bar: 50 μm. (C) SOX2 immunostaining identifies the prosensory domain within the embryonic cochlea. CPC localizations are indicated by yellow dashed circles. Scale bar: 50 μm. (D) Unsupervised clustering of E13.5 cochlear epithelial cells and progenitor-specific gene expression profiles.

Figure S2.

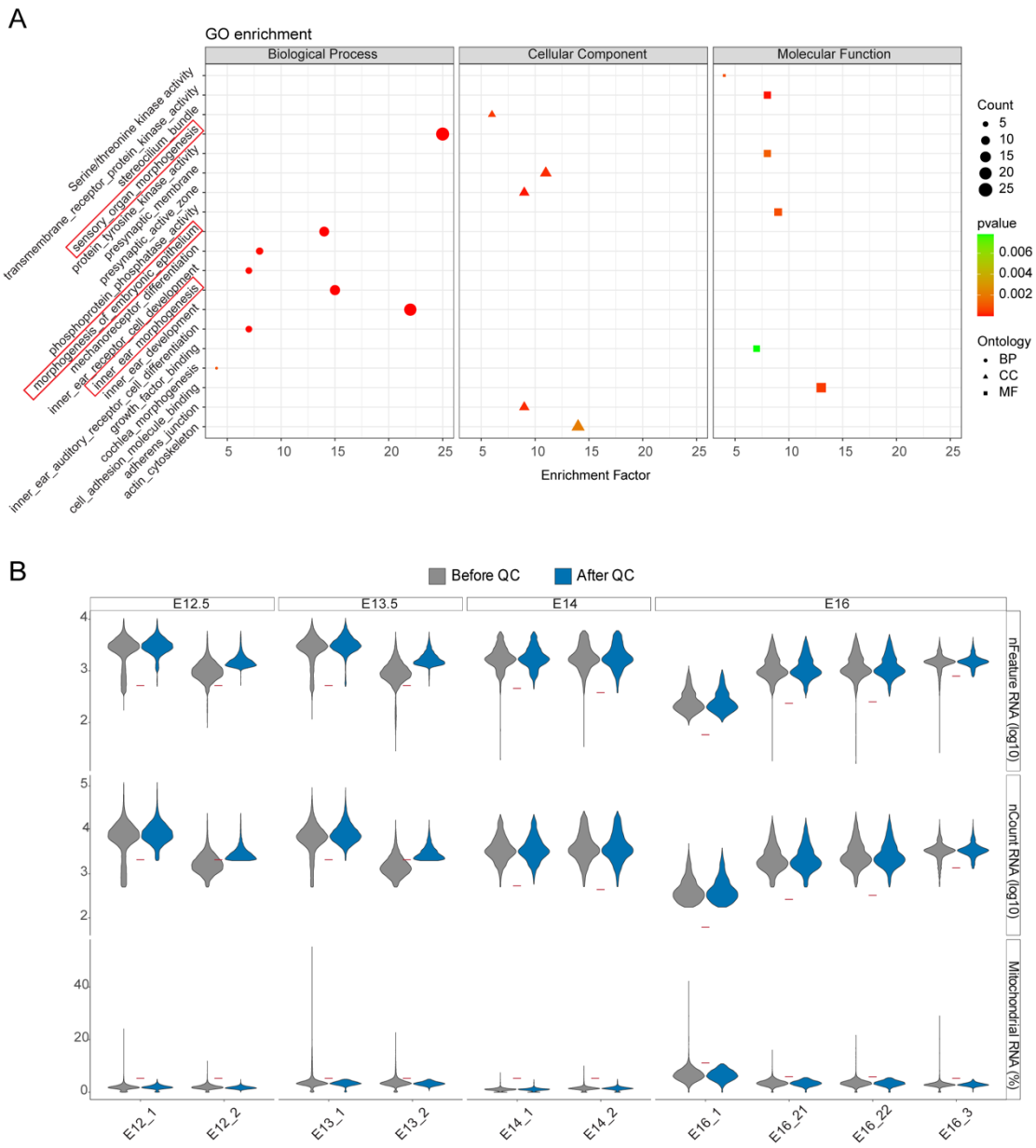


Figure S2. Functional enrichment analysis and quality control of single-cell RNA sequencing data.

(A) Gene ontology analysis reveals enrichment of cochlear morphogenesis-related genes in E12.5 CPCs. (B) Quality control metrics of single-cell RNA sequencing data across developmental stages. Violin plots showing the distribution of nFeature RNA (log10), nCount RNA (log10), and mitochondrial RNA percentage before (gray) and after (blue) quality control. Data are shown for each library across embryonic stages E12.5, E13.5, E14, and E16.

Figure S3.

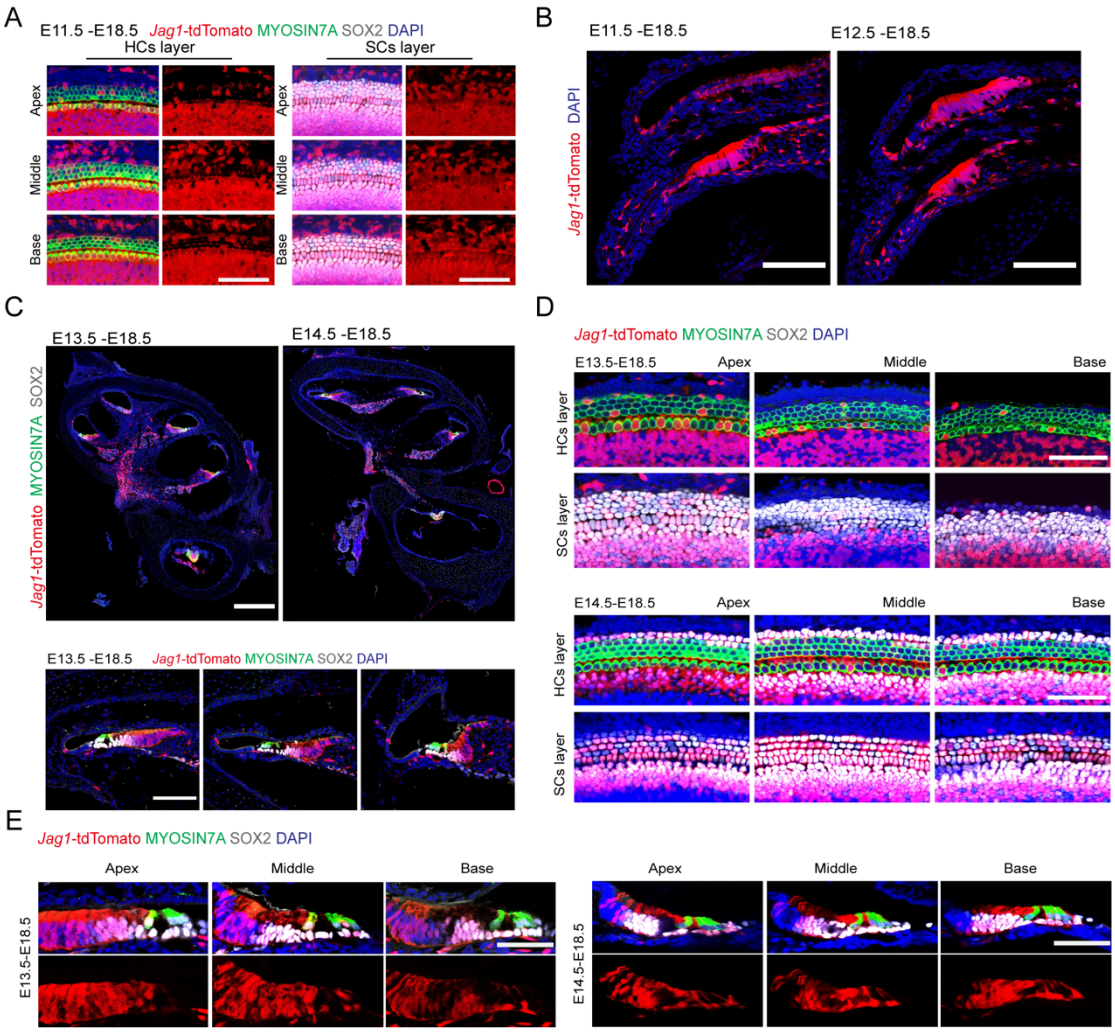


Figure S3. Lineage Tracing of *Jag1*$^{+}$ CPCs Using *Jag1*-iCreERT2; *Rosa26*-tdTomato Mice.

(A) Immunostaining for MYOSIN7A, SOX2, and DAPI in E18.5 cochlear epithelium following tamoxifen induction at E11.5. Scale bar: 50 μm. (B) *Jag1*$^{+}$ CPCs derived cells in E18.5 cochlear cross-section following tamoxifen induction at E11.5 or E12.5. Scale bar: 100 μm. (C) Distribution of *Jag1*$^{+}$ lineage-derived cells across inner ear tissues, including cochlear and vestibular epithelia and spiral ganglion. Scale bars: 200 μm (upper panel) and 50 μm (lower panel). (D, E) Immunostaining for MYOSIN7A, SOX2, and DAPI in E18.5 cochlear epithelium following tamoxifen induction at E13.5 or E14.5. Scale bars: 50 μm.

Figure S4.

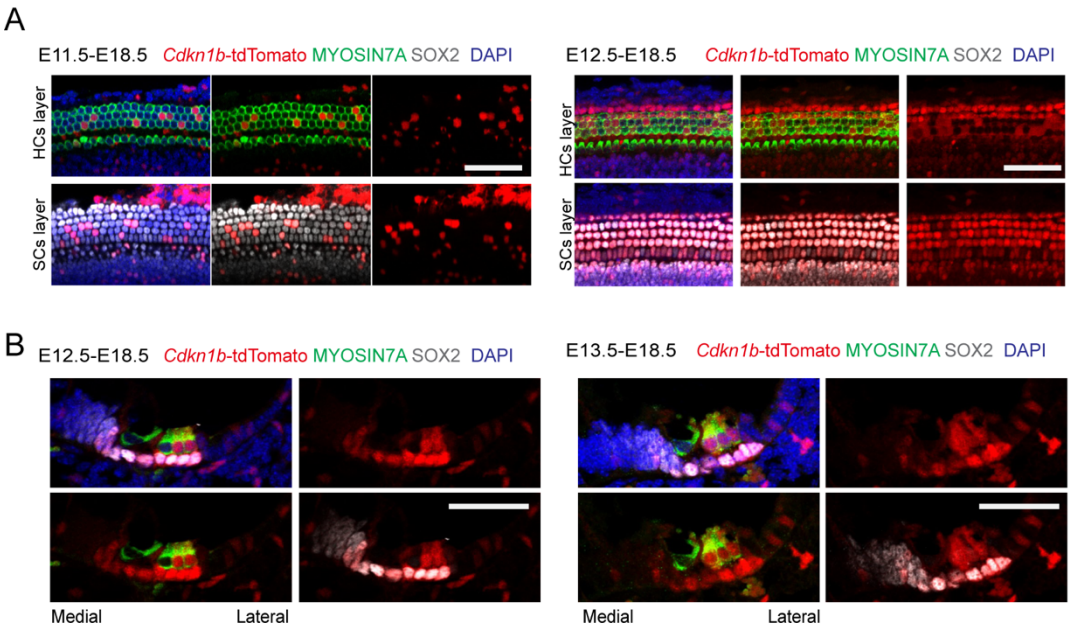


Figure S4. Lineage Tracing of *Cdkn1b*$^{+}$ CPCs Using *Cdkn1b*-iCreERT2; Rosa26-tdTomato Mice.

(A) Immunostaining for MYOSIN7A, SOX2, and DAPI in the middle turn of the E18.5 cochlear epithelium following tamoxifen induction at E11.5 and E12.5. Scale bar: 50 μm. (B) Immunostaining for MYOSIN7A, SOX2, and DAPI in E18.5 cochlear cross-section following tamoxifen induction at E12.5 and E13.5. Scale bar: 50 μm.

Figure S5.

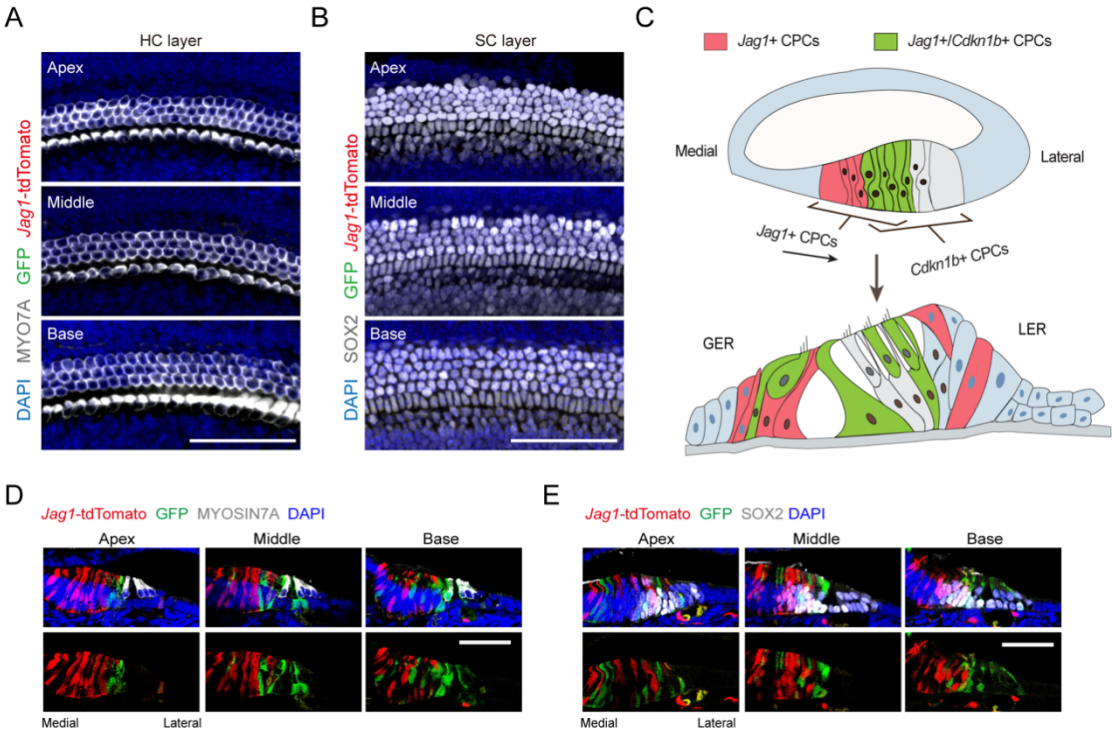


Figure S5. Dual-Recombinase Lineage Tracing of *Jag1*$^+$ and *Jag1*$^+$/*Cdkn1b*$^+$ CPCs Using *Jag1*-iCreERT2; *Cdkn1b*-Flpo; *Rosa26*-IS Mice.

(A, B) Representative immunofluorescence images of the cochlear epithelium showing the absence of GFP and tdTomato reporter signals in both the hair cell layer (A) and the supporting cell layer (B) without tamoxifen administration. Scale bar: 50 μm. (C) Expression patterns of *Jag1* and *Cdkn1b* in the prosensory epithelium with corresponding lineage-traced distributions of *Jag1*$^+$ and *Jag1*$^+$/*Cdkn1b*$^+$ CPCs in the organ of Corti. Scale bar: 50 μm. (D, E) Immunostaining for MYOSIN7A, SOX2, and DAPI in E18.5 cochlear epithelium after tamoxifen induction at E12.5, E13, and E13.5. Scale bar: 50 μm.

Figure S6.

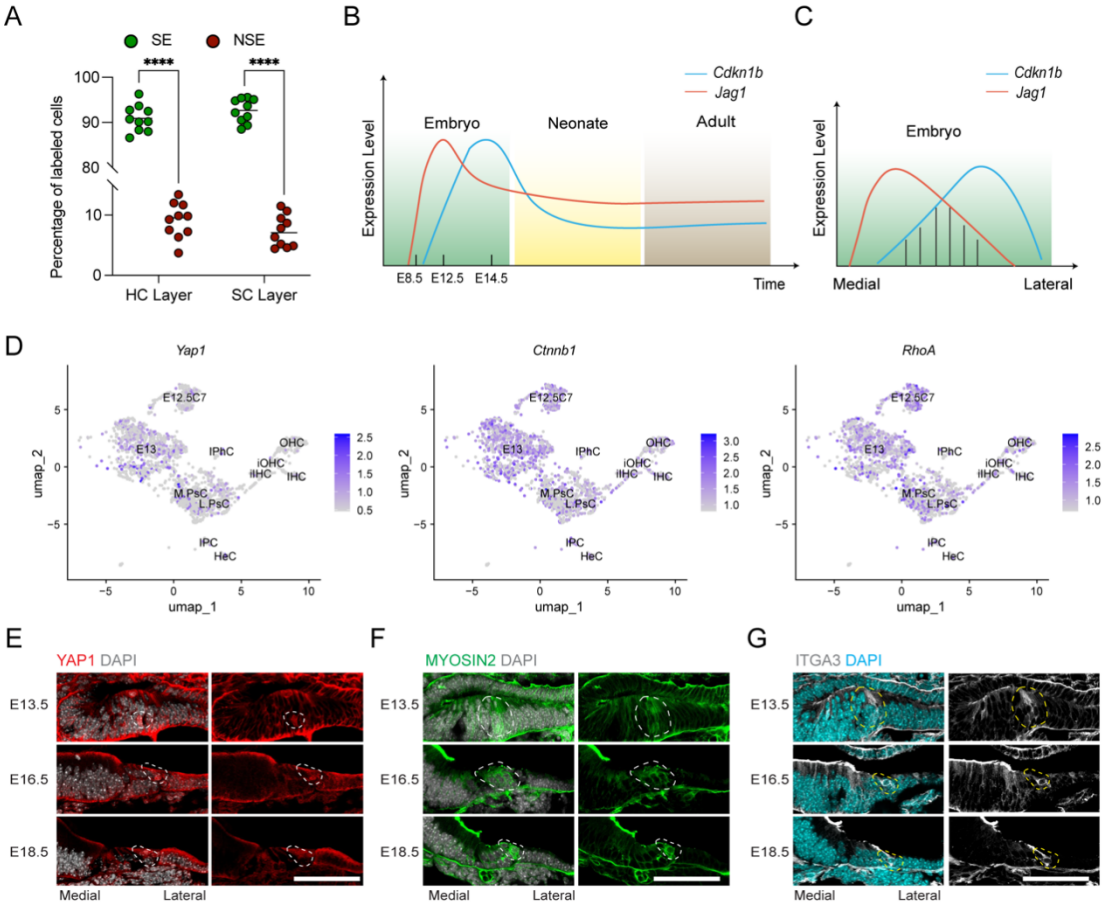


Figure S6. Expression of *Jag1*, *Cdkn1b*, and Mechanotransduction-Related Molecules During Cochlear Development.

(A) Percentage of GFP^{+} cells within sensory epithelium (SE) and non-sensory epithelium (NSE) in *Jag1*-iCreERT2; *Cdkn1b*-Flpo; Rosa26-IS mice (n = 10). (B) Temporal expression profiles of *Jag1* and *Cdkn1b* during cochlear development. (C) Spatial expression of *Jag1* and *Cdkn1b* along the medial–lateral axis of the cochlea. (D) Expression of mechanotransduction-related genes (*Yap1*, *Ctnnb1*, and *RhoA*) in developing cochlear cells. (E-G) Immunostaining of mechanotransduction-related proteins in the cochlear epithelium. The dashed circle highlights the expression domains of mechanotransduction components (YAP1, MYOSIN2, and ITGA3) in E13.5 CPCs and HeCs (E16.5 and E18.5). Scale bar: 50 μm. ****$p < 0.0001$ by Student's t test (A).

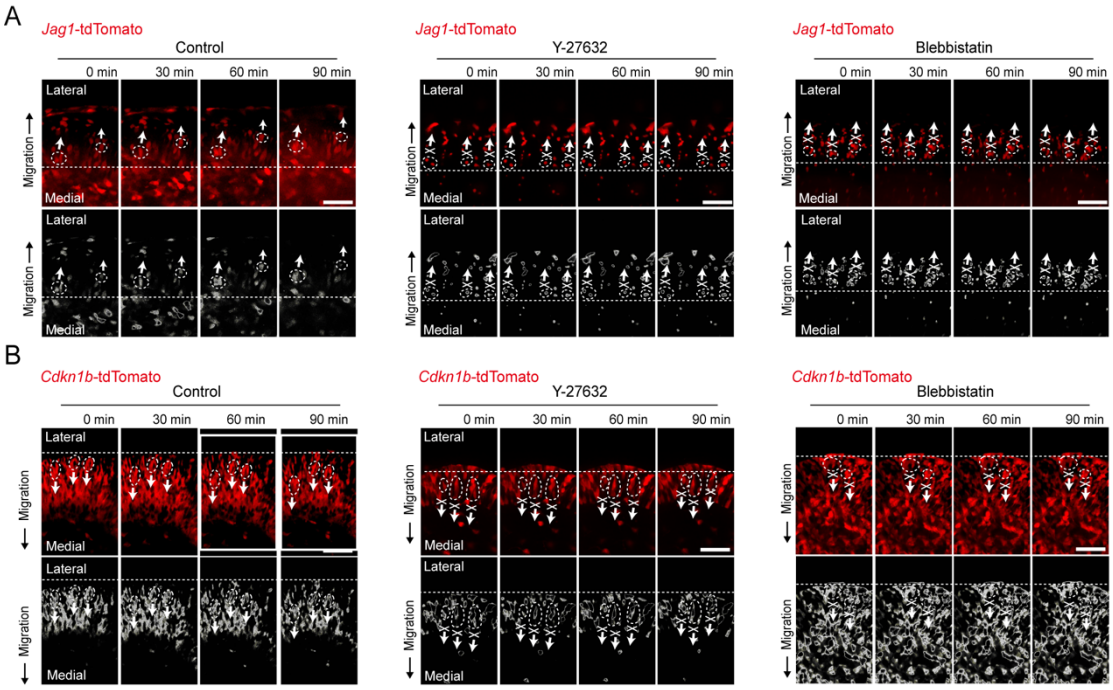


Figure S7. Rho/ROCK signaling and actomyosin contractility are required for CPC reciprocal migration.

(A) Representative time-lapse images of *Jag1*$^{+}$ CPCs in E14.5 cochlear prosensory explants treated with vehicle control, the ROCK inhibitor Y-27632 (10 μM), or the MYOSIN II inhibitor blebbistatin (10 μM). (B) Representative time-lapse images of *Cdkn1b*$^{+}$ CPCs in E15.5 cochlear prosensory explants under the same treatment conditions as in (A). For (A) and (B), dashed lines indicate the baseline; arrows indicate the direction of CPC migration. Scale bar: 50 μm.

Table 1. Primers for genotyping.

Gene	**Primer**
Jag1-iCreERT2 Common Forward	5′- AAACACCAGCAGAAAGTCCGCTTTG -3′
Jag1-iCreERT2 Wild type Reverse	5′- AGTGGAAGCCAGCTTGTCGAAACTT -3′
Jag1-iCreERT2 Mutant Reverse	5′- CTTCCTGACTTCATCAGAGGTGGCAT -3′
Cdkn1b-iCreERT2 Wild type Forward	5′- ACT TCT GTC AGC CAT TGT CGA T -3′
Cdkn1b-iCreERT2 Common Reverse	5′- GGG GTG CAA ATA CTG CAT TAT AGT CCC -3′
Cdkn1b-iCreERT2 Mutant Forward	5′-AAG AGA AGG ACC ATA TCC ACC GAG T-3′
Cdkn1b-Flpo Common Forward	5′- GCCTACTTCTGTCAGCCATTGT-3′
Cdkn1b-Flpo Wild type Reverse	5′- CCTCATTCTGATTCCACTTTAAGGTA-3′
Cdkn1b- Flpo Mutant Reverse	5′- TAGCTCCGCTTCCTCCGCCATG-3′
Rosa26-tdTomato WT Forward	5′- AAG GGA GCT GCA GTG GAG TA-3′
Rosa26-tdTomato WT Reverse	5′- CCG AAA ATC TGT GGG AAG TC-3′
Rosa26-tdTomato Mutant Forward	5′- GGC ATT AAA GCA GCG TAT CC-3′
Rosa26-tdTomato Mutant Reverse	5′- CTG TTC CTG TAC GGC ATG G-3′
Rosa26-IS RCE-Rosa1	5′- CCCAAAGTCGCTCTGAGTTGTTATC-3′
Rosa26-IS RCE-Rosa2	5′- GAAGGAGCGGGAGAAATGGATATG-3′
Rosa26-IS RCE-Cag3	5′- CCAGGCGGGCCATTTACCGTAAG -3′

Table 2. List of primary antibodies.

Antibodies	**Manufacturer**	**Cat Number**
Rabbit anti-MYO7A	Proteus BioSciences	25-6790
Goat anti-SOX2	R&D System	AF2018
Rabbit anti-KI67	Cell signaling technology	9129T
Mouse anti-V5	Abcam	ab27671
Mouse anti-HA	Merck	H9658-100UL
Rabbit anti-P27KIP1	Abcam	ab32034
Rabbit anti-JAG1	Abcam	ab109536
Mouse anti-P27KIP1	BD Biosciences	610241
Rabbit anti-YAP1	Cell signaling technology	14074T
Rabbit anti-MYOSIN2	Cell signaling technology	3403T
Rabbit anti-ITGA3	Proteintech	66070-1-Ig

Table 3. Single-cell RNA sequencing read depth and gene detection metrics.

Library	Identified cells	Mean reads/cell	Median genes/cell	Median UMIs/cell
E12_1	16,323	17,573	2,794	7,204
E12_2	13,393	3,527	982	1,635
E13_1	15,177	19,395	2,898	6,859
E13_2	13,064	4,226	919	1,410
E14_1	2,825	22,130	1,730	3,429
E14_2	4,005	26,265	1,767	3,712
E16_1	3,180	5,320	228	385
E16_21	4,643	27,174	1,042	1,986
E16_22	4,558	47,391	1,111	2,427
E16_3	4,783	44,366	1,489	3,353

Table 4. Single-cell RNA sequencing alignment efficiency and saturation metrics.

Library	**Valid barcode fraction**	**Reads inside cells fraction**	**Reliably mapped to transcriptome fraction**	**Sequencing saturation**
E12_1	98.0%	89.8%	83.0%	34.0%
E12_2	97.7%	87.8%	83.2%	21.7%
E13_1	97.5%	76.2%	82.5%	31.0%
E13_2	96.8%	74.4%	82.5%	31.7%
E14_1	95.2%	84.3%	84.2%	69.5%
E14_2	95.1%	88.2%	82.6%	70.8%
E16_1	65.4%	84.6%	81.6%	75.8%
E16_21	66.2%	86.3%	79.4%	75.5%
E16_22	94.8%	88.1%	79.3%	88.5%
E16_3	95.5%	93.9%	70.9%	87.1%

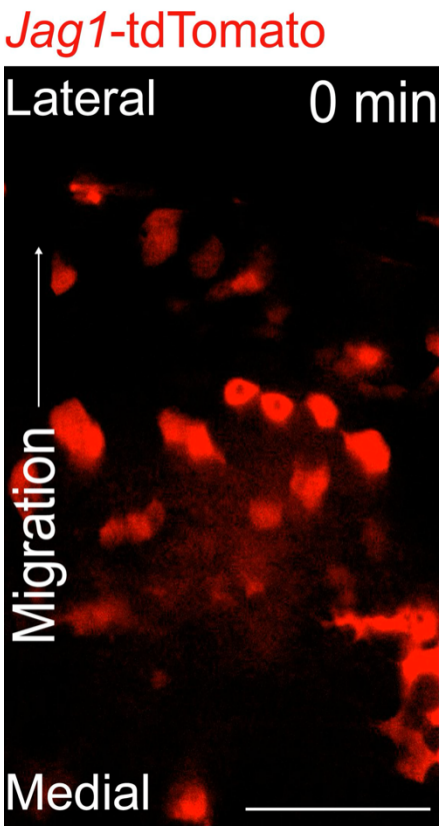
Table 5. Dynamic genes identified by pseudotime trajectory analysis.

Panel	Gene	Trajectory_FDR	Trajectory_amplitude_log1pCP10K	Specificity_FDR
Progenitor	Tbx2	5.62E-05	0.684651	9.44E-24
Progenitor	Jag1	0.09224	0.408985	4.61E-04
Progenitor	Mki67	2.10E-17	0.408535	1.54E-25
Progenitor	Ube2c	3.46E-17	1.263348	1.68E-57
Progenitor	Ube2t	1.04E-08	0.197776	3.96E-05
Progenitor	Foxg1	1.30E-13	0.545182	1.70E-41
Progenitor	Otogl	6.79E-12	1.074662	2.13E-41
Progenitor	Lin28b	2.51E-17	1.2704	2.45E-87
Progenitor	Rorb	2.81E-16	1.584448	1.26E-104
Progenitor	Otol1	4.64E-11	1.004959	1.17E-52
Progenitor	Clu	1.21E-09	1.738377	1.32E-48
Progenitor	Otog	3.18E-07	0.647709	1.46E-18
Progenitor	Lgr5	7.36E-05	0.531081	0.257777
Progenitor	Fst	5.43E-06	0.981361	5.92E-34
Progenitor	Cdkn1b	8.91E-08	0.504523	9.58E-18
Progenitor	Hey2	2.02E-10	0.692903	1.80E-46
Progenitor	Ikzf2	3.07E-13	0.708157	1.07E-48
Progenitor	Lgr4	1.41E-11	0.607272	5.50E-38
Progenitor	Ybx3	1.08E-17	1.519896	2.55E-139
Progenitor	Sox10	8.30E-15	1.009564	1.28E-63
Progenitor	Eya4	1.15E-11	0.883231	1.19E-74
Progenitor	Cmip	5.13E-09	0.351143	2.54E-09
Progenitor	Eya2	1.32E-13	0.543133	6.48E-45
HC	Espn	1.93E-21	1.298902	2.94E-26
HC	Cxcl14	1.08E-13	0.588307	3.69E-07
HC	Chrna9	1.54E-26	0.706061	1.01E-10

HC	Myo15	5.62E-27	0.758404	1.58E-10
HC	Acbd7	5.69E-26	1.724986	2.13E-29
HC	Myo6	2.05E-30	1.959763	2.70E-49
HC	Rbm24	2.09E-30	0.730008	5.96E-10
HC	Pvalb	2.08E-26	1.88356	5.92E-26
HC	Cdh23	1.27E-32	0.906067	1.06E-08
HC	Otof	2.55E-23	0.51334	1.37E-08
HC	Cib2	3.34E-34	2.400018	3.19E-75
HC	Tmprss3	6.02E-17	0.449463	0.008814
HC	Pcp4	2.18E-23	3.340873	2.24E-58
HC	Atoh1	1.58E-26	1.798716	1.28E-44
HC	Fgf8	4.08E-14	0.85481	5.94E-14
HC	Ccer2	1.95E-20	3.555673	1.16E-73
HC	Pou4f3	2.69E-24	2.343225	2.38E-83
HC	Calb2	3.41E-15	0.308209	0.118278
HC	Tmie	1.55E-21	0.55758	8.23E-08
HC	Chd7	9.04E-08	0.42233	0.014529
SC	Rgcc	3.46E-05	0.492412	3.62E-07
SC	Otoa	0.139311	0.039942	0.6619
SC	Bmp4	0.001708	0.279231	1.77E-10
SC	Jag1	0.050526	0.256531	1.32E-21
SC	Ednrb	0.069143	0.082504	0.007954
SC	Gjb2	2.21E-09	1.41683	4.94E-26
SC	Lfng	1.39E-09	0.421559	6.45E-06
SC	Npy	1.60E-10	0.916362	7.26E-62
SC	Gjb6	1.06E-05	0.20804	2.11E-13
SC	S100b	8.35E-08	0.154382	1.62E-07
SC	Hes5	3.89E-20	0.291113	1.12E-10

SC	Prss23	9.19E-09	0.48707	9.80E-17
SC	Gata2	6.16E-06	0.368401	1.41E-32
SC	Pmch	0.058491	0.048491	2.12E-17
SC	Stat3	5.45E-10	0.360745	0.412328
SC	Prox1	1.06E-10	0.474006	0.121414
SC	Dcn	6.52E-05	0.448611	1.45E-17

Video 1 (separate file). Tracing of *Jag1*$^{+}$ CPCs in developing cochlea epithelium.



Video 2 (separate file). Tracing of *Cdkn1b*$^{+}$ CPCs in developing cochlea epithelium.

